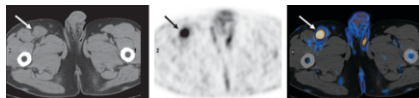
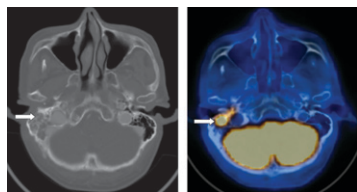
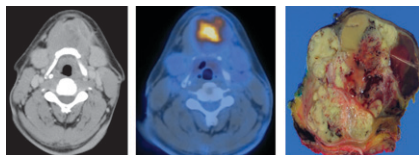


SPECT vs. PET in graft infection: Burrioni and colleagues review the gold standard of scintigraphy with radiolabeled white blood cells in vascular graft infection and the relative merits of PET and PET/CT in this indication. *Page 1227*

PET/CT in vascular graft infection: Keidar and colleagues assess the effectiveness of ^{18}F -FDG PET/CT in the diagnosis of vascular graft-related complications and in differentiation between graft and soft-tissue infection. *Page 1230*



PET/CT in salivary cancer: Jeong and colleagues compare the prognostic and treatment-planning abilities of ^{18}F -FDG PET/CT and contrast-enhanced CT in patients with high-grade salivary gland malignancies. *Page 1237*

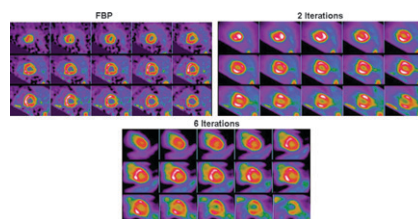


Novel PET tracer for GIST: Dimitrakopoulou-Strauss and colleagues describe PET studies with a ^{68}Ga -bombesin analog and ^{18}F -FDG in patients with gastrointestinal stromal tumors to investigate the effects of complementary receptor scintigraphy on diagnostic accuracy. *Page 1245*

PET/CT in recurrent esophageal cancer: Guo and colleagues report on the diagnostic and prognostic roles of ^{18}F -FDG PET/CT in

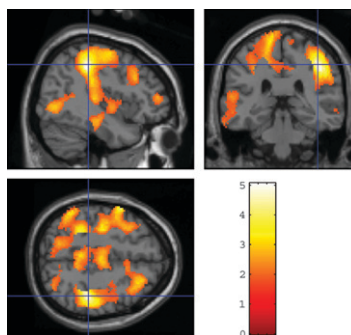
patients with suspected recurrence of esophageal squamous cell carcinoma after definitive treatment. *Page 1251*

Algorithms not interchangeable: Chen and colleagues provide data on the selection of reconstruction algorithms for ^{13}N - NH_3 PET estimation of quantitative myocardial blood flow. *Page 1259*



Receptor effect in breast cancer PET: Mavi and colleagues investigate correlations between ^{18}F -FDG uptake of primary breast cancer lesions and predictive and prognostic factors such as C-erbB-2, estrogen, and progesterone receptor states. *Page 1266*

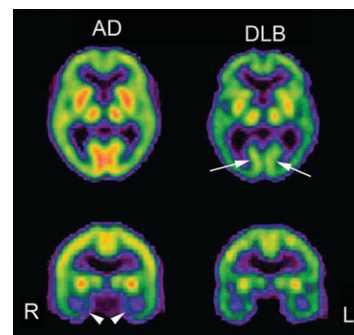
SPECT and rCBF in depression treatment: Kohn and colleagues use $^{99\text{m}}\text{Tc}$ -HMPAO SPECT to determine whether reversal of compromised regional cerebral blood flow in patients with major depressive disorder is dependant on the mode of antidepressant treatment. *Page 1273*



^{18}F -MPPF PET for longitudinal studies: Costes and colleagues assess the reliability and reproducibility of binding parameter quantification for this radiolabeled 5-HT $_1\text{A}$

receptor antagonist through a test-retest study over a long-term period. *Page 1279*

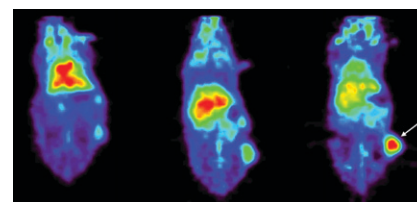
Advances in Alzheimer's assessment: Matsuda provides an educational overview of the role of neuroimaging in Alzheimer's disease, with a special focus on the utility of statistical analyses in brain perfusion SPECT, PET, and MRI techniques. *Page 1289*



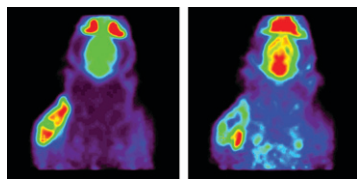
Monitoring myocardial therapy: Taki and colleagues evaluate $^{99\text{m}}\text{Tc}$ -annexin-V uptake in a rat model of ischemia and reperfusion to determine whether postconditioning or ischemic preconditioning suppress myocardial cell damage or apoptosis. *Page 1301*

^{18}F -FDG and mitochondrial membrane potential: Smith and Blaylock report on in vitro research in breast tumor cells to determine how the loss of mitochondrial membrane potential in apoptosis influences ^{18}F -FDG incorporation. *Page 1308*

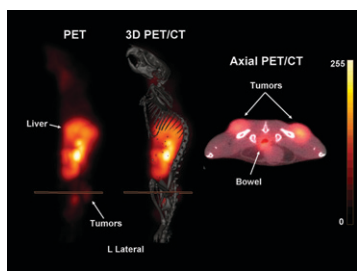
VEGF tumor imaging: Nagengast and colleagues describe the development of a radiolabeled humanized monoclonal antibody for noninvasive in vivo vascular endothelial growth factor visualization and quantification with ^{111}In and ^{89}Zr PET. *Page 1313*



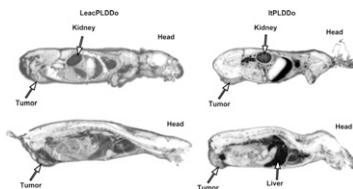
Lowered σ_1 binding after therapy: van Waarde and colleagues compare early changes in ^{11}C -SA4503 binding and ^{18}F -FDG uptake in gliomas after chemotherapy to evaluate the potential of a radiolabeled σ_1 -ligand for response monitoring. **Page 1320**



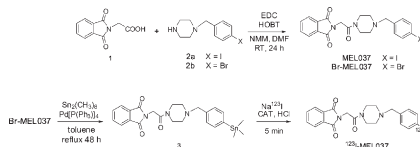
^{64}Cu -bombesin analogs for preclinical PET/CT: Garrison and colleagues report on studies in a mouse model of prostate cancer to determine whether the CB-TE2A chelation system could significantly improve the in vivo stability of ^{64}Cu -bombesin analogs. **Page 1327**



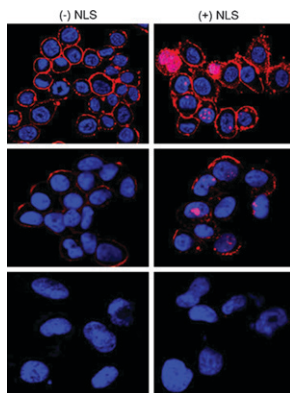
Novel carrier modules in lymphoma: DeNardo and colleagues characterize the pharmacokinetics of selective high-affinity ligand molecules that show promise as effective radioisotope carriers for molecular-based imaging and treatment of lymphoma. **Page 1338**



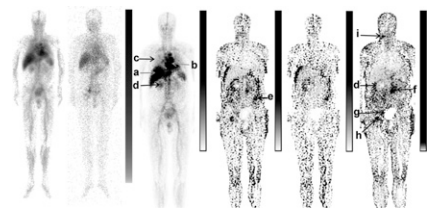
Imaging of melanoma metastases: Pham and colleagues describe mouse studies with a novel ^{123}I -labeled molecule for SPECT imaging and staging of metastatic dissemination of melanoma tumors and the potential for therapeutic applications. . . . **Page 1348**



^{111}In -trastuzumab and nuclear targeting: Costantini and colleagues evaluate the cytotoxicity and tumor-targeting properties of the monoclonal antibody trastuzumab modified with peptides harboring nuclear localization sequences and discuss the potential for radioimmunotherapeutic applications. . . **Page 1357**



Whole-body parametric imaging: Gleisner and colleagues detail a method for pharmacokinetic modeling of distributions of ^{111}In -labeled monoclonal antibodies on individual pixels of planar scintillation camera images. **Page 1369**



Solid-phase $^{99\text{m}}\text{Tc}$ preloading: Misra and colleagues introduce a multimeric, small-molecule radiotracer with high affinity to prostate-specific membrane antigen and describe its production through a solid-phase conversion of sodium $^{99\text{m}}\text{Tc}$ -pertechnetate to a general-purpose, reactive form. **Page 1379**

Chelate stability and ^{64}Cu : Eiblmaier and colleagues explore the question of whether ^{64}Cu localization to cell nuclei from internalizing, receptor-targeted radiopharmaceuticals is related to chelate stability. **Page 1390**

Journal impact factors: Currie and Wheat provide a general description of journal impact factor statistics in peer-reviewed nuclear medicine literature and discuss the implications, advantages, and shortcomings of these increasingly referenced metrics. **Page 1397**

ON THE COVER

^{68}Ga -BZH₃ may be helpful diagnostically in some patients with gastrointestinal stromal tumor. Here, ^{18}F -FDG shows hypermetabolic areas in the liver and stomach, CT shows hypodensity in the same areas, bombesin shows enhancement clearly in the liver but slightly in the stomach, and ^{18}F -FDG–bombesin fusion shows agreement between the tracers in the liver but not in the stomach. Histology revealed stomach tumor and liver metastasis.

See page 1248.

